IEEE Access
Multidisciplinary | Rapid Review | Open Access Journal

Received September 1, 2021, accepted September 20, 2021, date of publication September 23, 2021,
date of current version October 4, 2021.

Digital Object Identifier 10.1109/ACCESS.2021.3115472

Optically Instrumented Insole for Gait Plantar and Shear Force Monitoring

CÁTIA TAVARES[1,2,3], FLÁVIA LEITE[1,2,3], MARIA DE FÁTIMA DOMINGUES[3], (Member, IEEE), TIAGO PAIXÃO[1,2], NÉLIA ALBERTO[3], ANTÓNIO RAMOS[4], HUGO SILVA[5,6], (Senior Member, IEEE), AND PAULO FERNANDO DA COSTA ANTUNES[1,2,3]

[1]Department of Physics, University of Aveiro, Campus Universitário de Santiago, 3810-193 Aveiro, Portugal
[2] Institute for Nanostructures, Nanomodelling and Nanofabrication (I3N), University of Aveiro, Campus Universitário de Santiago, 3810-193 Aveiro, Portugal
[3]Instituto de Telecomunicações, University of Aveiro, Campus Universitário de Santiago, 3810-193 Aveiro, Portugal
[4]Centre for Mechanical Technology and Automation, Department of Mechanical Engineering, University of Aveiro, Campus Universitário de Santiago, 3810-193 Aveiro, Portugal
[5]Instituto Superior Técnico, Universidade de Lisboa (IST-UL), 1049-001 Lisbon, Portugal
[6]PLUX –Wireless Biosignals, S.A, 1050-059 Lisbon, Portugal

Corresponding authors: Cátia Tavares (catia.tavares@ua.pt) and M. Fátima Domingues (fatima.domingues@ua.pt)

This work was supported in part by Fundação para a Ciência e a Tecnologia – Ministério da Ciência, Tecnologia e Ensino Superior (FCT/MCTES) and Fundação para a Ciência e a Tecnologia / Ministério da Educação e Ciência (FCT/MEC) through National Funds and in part by EU Funds under Project UIDB/50008/2020-UIDP/50008/2020 and Project X-0005-AV-20-NICE-HOME. The work of Maria de Fátima Domingues and Nélia Alberto was supported in part by FEDER–PT2020 Partnership Agreement for the Scientific Actions REACT and PREDICT under Project UID/EEA/50008/2019 FCT. The work of Cátia Tavares supported by Fundação para a Ciência e Tecnologia (FCT) under Grant PD/BD/142787/2018.

ABSTRACT In this work, a fiber Bragg gratings (FBGs) based sensing insole, capable of simultaneously measure plantar force (PF) and shear force (SF) is proposed. The insole has four measuring points, strategically located for a full gait analysis. Each sensing point contains a sensor-cell which consists of a polylactic acid (PLA) structure, covered by an epoxy resin layer, and crossed by one optical fiber with two FBGs, FBG1 and FBG2, respectively. Due to the specific design of the system, the FBG1 is sensitive to both forces (with higher sensitivity to the PF), while the FBG2 is designed to detect only the SF. The instrumented insole was tested during static and gait exercises, and the results, obtained for the PF and SF monitoring, were according to those theoretically expected.

INDEX TERMS Foot plantar sensor, gait cycle anomalies, multiplexed fiber Bragg gratings, pressure ulcers, shear force sensor.

I. INTRODUCTION

With the progressive increase in life expectancy, a continuous monitoring of the aging citizens' health is a necessary requirement to ensure a healthy life [1]. Everyone wants to improve life quality, making the development of devices to monitor the physical capabilities essential to ensure that they are not weakened, or, when this happens, that any prescribed rehabilitation treatment is being done in a correct way and is being effective [2]. The advances in research areas like e-Health are driven by the purpose of providing solutions (including the sensing systems) that increase the quality of life of patients, as well as the necessary help to medical staff in the early diagnosis of anomalies. These sensing systems and e-Health enablers must be capable to help elder generations and patients with chronic illness to live an active life, without compromising their daily routines. To improve the quality of life of citizens with reduced mobility, our research team has been working in different practical optical fiber-based solutions for the continuous remote monitoring of patients' health [3]–[5].

The motivation for this work is to develop a fiber optic sensor system to detect abnormalities in the gait cycle that may be related to serious pathologies in the spine, as well as the detection of warning signals related to the appearance of pressure ulcers in the feet. These sensors can also be used in rehabilitation aids, like in the so-called exoskeletons.

This paper reports the optimization of a fiber Bragg gratings (FBGs) based device able to measure plantar force (PF) and shear force (SF). The proposed solution, designed as sensor-cell, is a polylactic acid (PLA) structure, covered by an epoxy resin layer and crossed by an optical fiber with two inscribed FBGs (FBG1 and FBG2). For the insole instrumentation, this sensor-cell was replicated, and positioned at four key points for the foot plantar forces analysis.

The associate editor coordinating the review of this manuscript and approving it for publication was Sukhdev Roy.

Pressure ulcers are localized lesions in the skin, or underlying tissues, that appear due to the decrease of the blood circulation inflicted by an increased pressure in specific areas of the body [6]. According to the study reported in [7], the average hospital treatment costs associated with stage IV pressure ulcers and related complications were $129,248 for hospital-acquired ulcers during 1 admission, and $124,327 for community-acquired ulcers over an average of 4 admissions [7]. Beyond their treatment financial cost, the untreated (or lately detected) pressure ulcers can also lead to limb amputations or even death of the patients.

As this serious pathology is commonly related to the foot, the existence of devices (typically insoles) able to predict its development in an early stage is of the utmost importance [8]. In that way, the device developed by our team aims to help in such early detection, since it is able to monitor the two fundamental parameters for the appearance and worsening of pressure ulcers: the foot plantar and shear forces [9]–[11]. The foot plantar force (PF) consists on the vertical reaction of the ground to the patient weight, and the shear force (SF) is related with the horizontal forces between the foot and the ground, and often referred in many published works as the responsible for this pathology [8].

Several authors highlight feet areas such as heel, midfoot, first metatarsal and hallux as the key points for the plantar and shear monitoring [12]–[14]. The typical distribution of PF and SF is depicted in Fig. 1, where the blue regions correspond to the areas with lower applied force, and the red ones are the areas where higher values of force are expected. In this figure, the four key points (black dots) where the sensor-cells were positioned are also identified. These points correspond to the expected higher values of PF and SF, and, therefore, the areas with more predisposition to the appearance of pressure ulcers.

FIGURE 1. Typical plantar and shear forces distribution in the foot, with the areas with higher (red) and lower (blue) forces. Identification of the sensor-cells position (black dots).

In the sensor market, there are many electronic devices available for the analysis of plantar pressure, such as pressure distribution platforms, imaging technologies with image processing software, and in-shoe systems. These solutions are generally equipped with piezoelectric and/or piezoresistive sensors and capacitive sensors [15], [16]. All these are electronic solutions, possessing relevant disadvantages that can potentially be mitigated by optical fiber technology. Furthermore, the solutions to simultaneously monitor shear and plantar forces are scarce and financially costly.

Optical fiber sensors (OFS) have been widely used into different areas, and in the last years its application in the biomedical fields has been greatly explored [17]. OFS are used for temperature control during several surgical procedures [18]; very low pressure levels for intracapillary measurements [19], medium pressure levels in finger interactive forces monitoring [20], and for higher pressure levels such as the pressure exerted by the body human [2], [3]. They have also been used for heart [21] and respiratory rate measuring [22], among others. When compared to their electronic counterparts, the advantages of these type of sensors include immunity to electromagnetic interferences, the ability to multiplex several sensors in a single optical fiber, and the possibility to be used in the presence of humidity without any special encapsulation, since no electric current is needed at the measurement point, making them intrinsically safer [17]. Also, due to its high accuracy and resolution, it is possible to achieve a level of detail in the deformation process, that the electronic sensors lack.

The monitoring of the vertical and tangential forces in biomedical applications, like analysis of plantar forces, or prosthetic applications, using OFS with FBG has also been considerably investigated.

In 2000, Koulaxouzidis *et al.* presented the first tangential and vertical forces sensor for physiological measurements. Nevertheless, the sensor was quite complex since it was composed by three FBGs embedded in a rubber block in three different orientations. When subjected to forces, the material is deformed, and consequently a variation on the reflected Bragg wavelength is observed [23]. Later, in 2013, Zhu's team presented a similar sensor, however they used two polymer FBGs (PFBGs) embedded in polydimethylsiloxanes (PDMS) block [24]. In 2016, Chethana *et al.* presented a 3D force measurement platform, based on several FBG sensors [25]. Later, it was reported the use of a cork insole with an FBG network [26] and PFBG network [27] sensors located at key points for the analysis of vertical force during gait. In 2018, our research group proposed a biaxial optical fiber sensor with two FBGs, using only one optical fiber, for simultaneous shear stress and vertical pressure monitoring [28]. Months later, the same research group reported the application of these sensors in an insole to monitor these same parameters in five different zones in the sole of the foot, to prevent/diagnose diabetic feet and disturbances in the synchronization of the lower limbs [29]. Each of these sensor-cells was composed by cork, PLA, epoxy resin and two in-line FBGs recorded on a single optical fiber [28], [29]. In the following year, the same authors proposed a bio-inspired cell-sensor capable of measuring the same physical parameters, but with a simpler production process, due to the use of a 3D printer to make the sensor-cell body, and without cork [30]. In 2020, Mai *et al.* proposed a similar solution, with the same working principle to fulfill the same purpose, but with two

sensor-cells and two distinct optical fibers: one to measure normal force, and the other to measure shear force [31].

Concerning to the prosthetic application, in 2017, an FBG-instrumented prosthetic silicone liner that provides cushioning for the residual limb and can successfully measure interface pressures inside prosthetic sockets of lower-limb amputees was proposed [32]. The liner is made of two silicone layers between which twelve FBG sensors were embedded at locations of clinical interest to measure pressure. A year later, it was reported the use of FBGs embedded into a carbon fiber reinforced polymer transtibial prosthesis to evaluate the user's gait, and its own performance [33]. The FBGs were positioned vertically and horizontally within the structure, and they have been used for load and strain force evaluation during real-time experiments with a candidate at different speeds on a treadmill. In 2019, a novel method to simultaneously measure the normal and shear strains using two FBGs sensors embedded into a foam liner that sits at the prosthetic interface was proposed [34]. The results show a very good agreement of measured normal and shear strains for loads below 20 N.

With this paper, we propose a new instrumented insole capable of simultaneously measuring plantar and shear forces at the same point of analysis. There is only one published work that fulfills the same purpose [29], however it presents some complexity of production due to the manual cutting of all the pieces involved in the sensor-cell production (pieces of only a few millimeters in dimension). So, we are now presenting a new sensor-cell design that reduces the production complexity, since only two materials are used and fewer manual production steps are involved, due to the use of 3D printing to produce the body of the sensor-cell and the base of the insole. With this proposed configuration, a higher ratio between each direction sensitivity was obtained, which is less prone to cross sensitivity effects.

This paper is organized in 5 sections: Section I is the introduction; Section II presents the FBG sensing principle; Section III focuses on the sensor-cell design, simulations and experimental characterization; Section IV shows the implementation of the sensor-cells on the insole and their performance during static and dynamic tests; Section V presents the overall device architecture; and Section VI outlines the main conclusions.

II. FBG SENSING PRINCIPLE

FBGs are produced by laterally exposing the optical fiber to a periodic pattern of, typically, an UV light. After exposure, they present a periodic perturbation in the refractive index of the fiber core, which is sensitive to external perturbations, such as temperature and strain variations. When an optical fiber containing an FBG is illuminated by a broadband light source, only a small set of wavelengths that meet the Bragg condition are reflected, being all the others transmitted. The Bragg condition is given by the following equation:

$$\lambda_B = 2n_{eff}\,\Lambda \tag{1}$$

where λ_B is the reflected Bragg wavelength, n_{eff} is the effective refractive index of the optical fiber core, and Λ is the grating period.

Any temperature (ΔT) and/or strain (Δl) variations will be translated in a Bragg wavelength shift ($\Delta\lambda_B$) in accordance with the following equation:

$$\begin{aligned}\Delta\lambda_B &= \Delta\lambda_{B,\iota} + \Delta\lambda_{B,T}\\ \Delta\lambda_B &= 2\left(\Lambda\frac{\partial n_{eff}}{\partial l} + n_{eff}\frac{\partial\Lambda}{\partial l}\right)\Delta l\\ &\quad + 2\left(\Lambda\frac{\partial n_{eff}}{\partial T} + n_{eff}\frac{\partial\Lambda}{\partial T}\right)\Delta T\\ \Delta\lambda_B &= \mathrm{S}_l\Delta l + \mathrm{S}_T\Delta T\end{aligned} \tag{2}$$

where the first term is the strain induced Bragg wavelength shift, and the last the thermal effect on the same parameter. S_l and S_T represent the strain and temperature sensitivity coefficients of the FBG, respectively.

In this work, each sensor-cell was produced with two in-line FBGs separated by 9.5 mm. The FBGs were inscribed into a photosensitive optical fiber (GF1 Thorlabs), using a pulsed Q-switched Nd: YAG laser system (LOTIS TII LS-2137U Laser), lasing at the fourth harmonic (266 nm). The FBGs were recorded through the phase mask technique, employing a laser pump energy of 25 J, a repetition rate of 10 Hz, and an exposure time of ∼1 min.

III. SENSOR-CELL DEVELOPMENT

A. DESIGN AND PRODUCTION

In our previously work [29], a complex sensor-cell production was used, involving three different materials and several manual production steps. The complex assembly methodologies make it difficult to replicate the sensor-cells, and therefore it adds a higher probability of errors in its construction and implementation feedback.

The present work intends to be a step forward from the previous sensing system, with a sensor-cell design providing an alternative solution that overcomes these two disadvantages. For that, the sensor-cell was designed to be printed in PLA on a 3D printer (Ultimaker 3D Extended), to facilitate the production process, to guarantee better reproducibility conditions, and to ensure the discrimination of the plantar and shear forces, with one of the two FBGs being only sensitive to the shear force.

Each sensor-cell is composed by an optical fiber (represented in green color in Fig. 2) containing two in-line FBGs, which were incorporated into a PLA piece (in blue color in the Fig. 2) and epoxy resin to protect the cell and to fill a cavity, which is within the zone 1 (in red color in Fig. 2).

The cell's base is composed by two zones: zone 1, which contains the cavity designed to accommodate the FBG mostly sensitive to vertical force (FBG1), while zone 2 contains the FBG that should be sensitive only to shear force (FBG2) (Fig. 2a). This sensor-cell has a dimension of 19.00 mm × 8.00 mm × 5.00 mm and a hole along its entire length at a height of 2.70 mm from the base, with a diameter of 0.80 mm

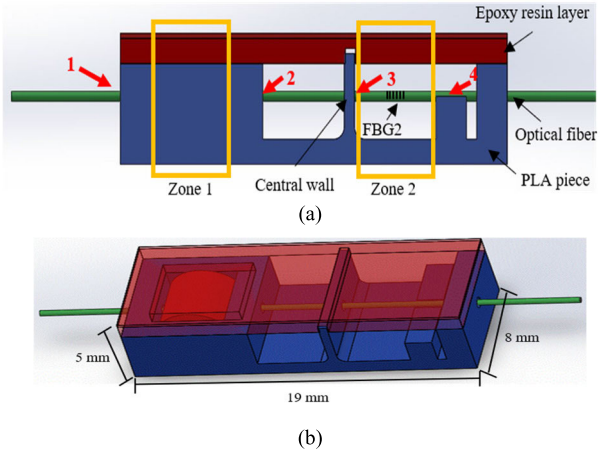

FIGURE 2. Sensor-cell design with the evidence of the materials and zones (a), and dimensions (b).

for the fiber allocation (Fig. 2b). The central wall, limiting zone 2, has a height of 4.20 mm (to be anchored in the epoxy top layer), a thickness of 0.90 mm and a curvature with the connection to its base with a radius of 0.75 mm. Such dimensions allow its longitudinal movement but constrains its vertical and transversal ones. These dimensions were set based on the theoretical analysis described in the following section.

The optical fiber containing the two FBGs was first placed in the PLA piece, with the FBG1 positioned in the middle of the cavity (zone 1), and the FBG2 (sensitive to shear) located between the central wall and the small wall. Then, the optical fiber was glued to the PLA at four points (1, 2, 3 and 4 identified in red in Fig. 2a: first between the first and the second points; second, between the third and the fourth points. In the second bonding, between points 3 and 4, the optical fiber was tensioned (with a tension corresponding to a Bragg wavelength shift of around 1 nm). Between the second and third points, the fiber is not tensioned, so that the forces undergo by FBG1 do not influence the forces applied in FBG2, and vice-versa. The aim of the lower wall between the points 3 and 4 is to support the optical fiber between those fixed points. After the fiber bonding process, the cavity of the zone 1 was filled with epoxy resin (Advanced from Liquid Lens^{TM}), represented in red in Fig. 2. Lastly, a resin layer with a thickness of approximately 1 mm was placed over all the PLA piece. The main function of this layer is to provide to the sensor-cell a protection in terms of physical integrity, and to allow the FBG2 to be sensitive to the shear forces felt on its surface. This second purpose is only possible because this layer has a groove to fit the central wall of the base. In other words, the surface of the sensor-cell when exposed to tangential forces (shear) will move the central wall, which is thin enough to undergo slight lateral displacements, but thick enough not to break.

As the FBG1 was embedded in the resin, it will be sensitive to all events to which the resin is subjected, namely both plantar and shear forces.

The shear felt on the insoles always behaves in the same way: runs from the toes towards the heel. Therefore, the sensor-cell will be placed on the insole so that the shear occurs in the direction from FBG1 to FBG2. Due to the cell design, it is expected that the FBG1 will be stretched in the presence of PF, whereas for FBG2 this happens for the case of SF, since it was glued to a wall that is only expected to undergo shear.

Previous works report that the maximum pressure exerted on the sole of the foot during walking is about 0.27 MPa [11], but once an FBG embedded in epoxy resin has a much higher compression limit, about 1.57 MPa [35], our sensor-cell is a good solution for the pressure range to which an insole is exposed during walking.

B. FINITE ELEMENT SIMULATION

The sensor-cell behavior was simulated using finite element modeling with "SolidWorks Simulation" software, considering the expected maxima values of plantar and shear forces reported in the literature, of 42 N and 8 N, respectively [11]. This simulation allowed to visualizing and understand the behavior of the sensor-cell, and to optimize the characteristics of the central wall. From the results presented in Fig. 3 we can conclude that, for a plantar force of 42 N, the cavity 1, and consequently, the FBG1 suffer the most deformation, while the FBG2 in zone 2 does not show significant changes (the presence of a greenish color allows to predict that there is only a very small movement of the central wall).

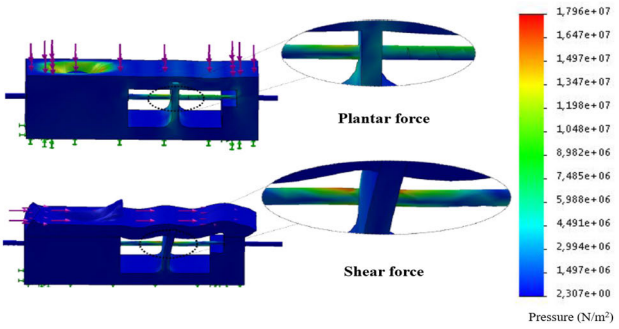

FIGURE 3. Simulation results of the behavior of the sensor-cell when a plantar and shear forces are applied.

For the case of a shear force of 8 N, it is shown that the resin at the top of the cavity 1 moves significantly, so it is expected that the FBG1 is sensitive to this force. In relation to FBG2, it is also observed that the optical fiber near the central wall undergoes some tension (presence of red color). So, as expected, both FBGs will be sensitive to shear force (Fig. 3). Several sensor-cells, with different central wall dimensions, were also simulated to attain the most suitable wall characteristics that should induce a greater sensitivity to shear forces, without compromising the wall structure. The results revealed that the wall should have the following dimensions: 4.20 mm of height, 0.90 mm of thickness and a curvature radius with the base of 0.75 mm.

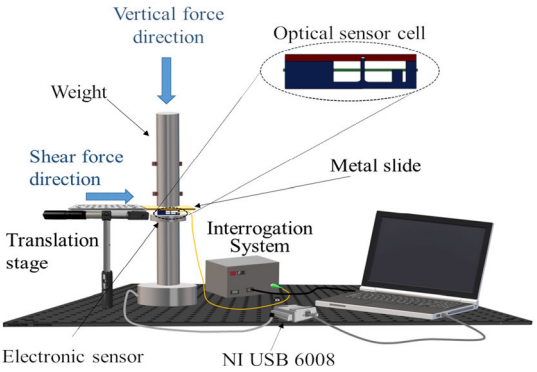

FIGURE 4. Schematic representation of the experimental setup used to calibrate the FBGs.

C. EXPERIMENTAL CHARACTERIZATION

Prior to the sensor-cell application, it is crucial to calibrate each FBG independently for each of the forces, aiming to convert its wavelength shift into the respective force value applied to the sensor-cell. So, for the calibration, an electronic multiaxial force sensor (LFX-A-1KN Kyowa) was used. The sensor-cell was fixed to the electronic sensor, with the aid of double-sided tape, allowing the forces to be felt simultaneously in both devices (over both electronic sensor and sensor-cell). The data from the electronic sensor was acquired through an analog-to-digital converter (ADC) (USB6008, National Instruments), while the optical signal provided by the sensor-cell was acquired by an optical interrogator (I-Mon512, Ibsen), with an acquisition rate of 912 Hz. A schematic representation of the implemented experimental setup is depicted in Fig. 4.

To calibrate the sensor-cell to shear force, a metal plate was placed between the sensor-cell and a weight, which was properly tightened, preventing the movement over the plate. The plate was then pushed horizontally using a micrometric screw (translation stage) (Fig. 4). Thus, the plate slid parallel to the surface of the sensors (optical and electronic), causing SF (shear force) in both sensors, while the PF (plantar force) remained constant ($\Delta PF \approx 0$ N). For the vertical force calibration, several weights were used, in order to vary the force that was applied vertically in the sensor-cell, while the shear force was set constant ($\Delta SF \approx 0$ N).

During the PF and SF calibrations, the data from both sensors were simultaneously acquired for later comparison.

Figure 5 presents the data acquired by the reference electronic and optical devices, during the PF and SF calibrations. In Figs. 5a and 5b there is an increase (in module) of the force exerted on the sensor due to the placement of the weights over time and, as predicted, the SF remained constant ($\Delta SF \approx 0$ N). In the case of the optical sensor, this increase is observed by the Bragg wavelength shift on the two FBGs, being this behavior more accentuated for the FBG1, as expected (Fig. 5b).

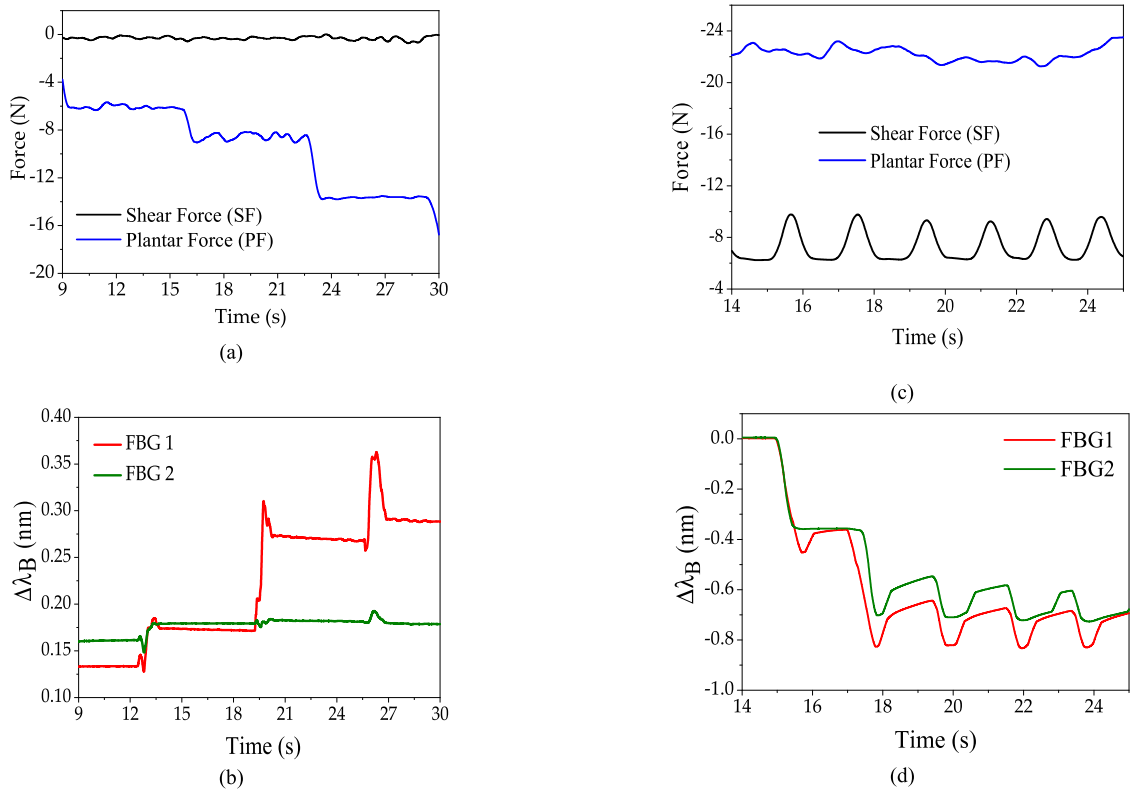

FIGURE 5. Data acquired by the electronic ((a) and (c)) and optical ((b) and (d)) devices, for the PF ((a) and (b)) and SF ((c) and (d)) forces.

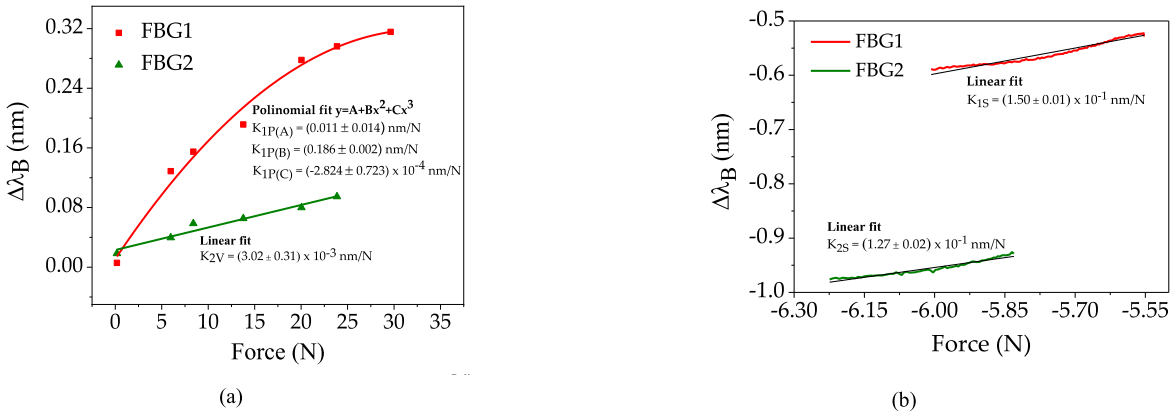

FIGURE 6. Bragg wavelengths shift as function of the PF (a) and SF (b), and their respective linear and/or polynomial fitting curves.

In the data acquired during the shear calibration (Figs. 5c and 5d), the periodic variations induced by the micrometer screw are observed in the response of both sensors. On the electronic device, one turn on the screw (equivalent to pushing the metal plate for a short period of time) corresponds to the zone of increased force, followed by a moment of relaxation (decrease force), until the screw is turned again. As the plantar force on the cell was kept constant throughout this procedure, the data acquired by the electronic sensor shows very small oscillations.

Aiming at the determination of the FBG1 and FBG2 sensitivities to plantar and shear forces, the data acquired with the electronic and optical sensors were correlated, being the results present in the Fig. 6.

The graphs show that there is a linear dependence of the FBG1 and FBG2 responses with the applied shear forces. When applying a vertical force, it was verified that the FBG2 present a linear response, whereas FBG1 has a polynomial behavior (Fig. 6a), mainly due to the elastic response of the resin. The sensitivities obtained for each of the FBGs to the plantar force (K_{1P} and K_{2P}) and to the shear force (K_{1S} and K_{2S}) are summarized in Table 1. Additionally, for the polynomial fit to the FBG1 data we have the coefficients A, B and C instead of just a single sensitivity value (called $K_{1P(A)}$, $K_{1P(B)}$ and $K_{1P(C)}$, respectively).

TABLE 1. Sensitivity coefficients (values in nm/N).

	PF	SF
FBG1	$K_{1P(A)}$= 0.011±0.014 $K_{1P(B)}$= 0.186±0.002 $K_{1P(C)}$= -2.824±0.723 x 10^{-4}	K_{1S}= (1.500±0.010) x 10^{-1}
FBG2	K_{2P}= (3.020±0.310) x 10^{-3}	K_{2S}= (1.270±0.020) x 10^{-1}

The wavelength shift of the FBGs can be related with the plantar (ΔF_P) and shear forces (ΔF_S) through the following system of equations:

$$\begin{aligned}\Delta\lambda_{B1} &= \left(K_{1P(A)} + K_{1P(B)}.\Delta F_P + K_{1P(C)}.\Delta F_P^2\right) + K_{1S}.\Delta F_S \\ \Delta\lambda_{B2} &= K_{2P}.\Delta F_P + K_{2S}.\Delta F_S \end{aligned} \quad (3)$$

After applying Equation (3) to the raw data of $\Delta\lambda_B$ values obtained from the optical device, it was possible to calculate the values of the corresponding force. Figure 7 compares the response of the optical and the electronic sensors (in terms of normalized forces), when the PF and SF were simultaneously applied. In Fig. 7a is presented the plantar force, while Fig. 7b depicts the shear force. The difference between the curves has a normalized mean square error of $RMSE_P = 0.119$ for the plantar force, and $RMSE_S = 0.153$ for the shear force.

The sensor-cell's response time and measurement repeatability were tested (Fig. 8) by placing and removing an identical load 10 times over a sensor-cell. From this test, it can be concluded that the average response time is 0.38 s for load applications and 0.44 s for load relief, and the sensor-cell present a negligible hysteresis, since it recovers its optical signal characteristics after several loading cycles.

IV. IMPLEMENTATION OF THE SENSOR-CELLS IN AN INSOLE

The insole was designed for the incorporation of four sensor-cells, being its structure printed in PLA on the 3D printer (BCN3D - R19). The four sensor-cells were strategically positioned at key points for the analysis of the gait cycle, namely heel (P1), 1st metatarsal (P2), hallux (P3) and 4th and 5th metatarsus area (P4), Fig. 9. Due to the multiplexing capabilities of FBGs, the number of sensor-cells can be increased, and their position can be adjusted according to the user's requirements. Here, we only present a proof-of-concept of the developed design, with four sensor-cells, placed at the locations more prone to develop ulcers due to the shear movement.

The insole contains eight FBGs inscribed into GF1 Nufern's photosensitive optical fiber multiplexed into two optical fiber cables, with Bragg wavelengths ranging from 1530 to

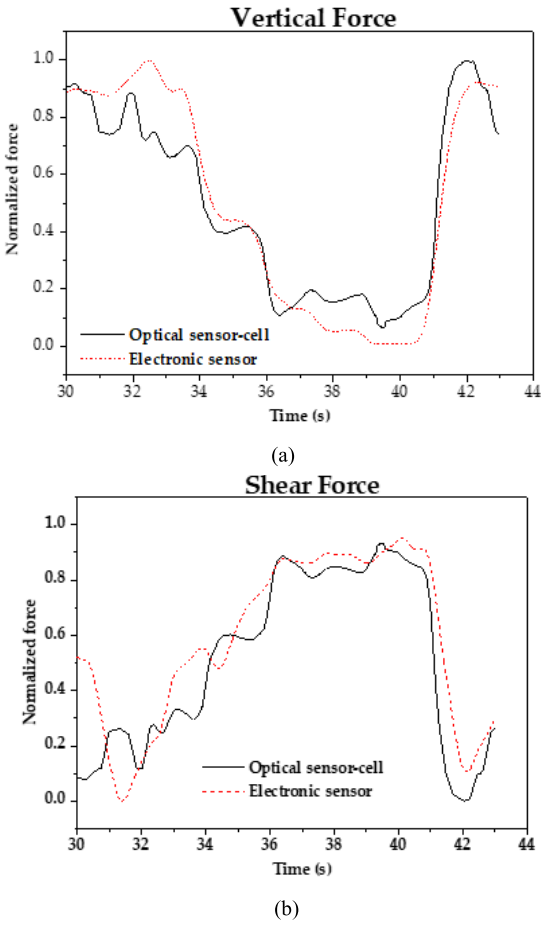

FIGURE 7. Comparison of the normalized plantar (a) and shear (b) forces, acquired with the electronic device and the developed optical sensor.

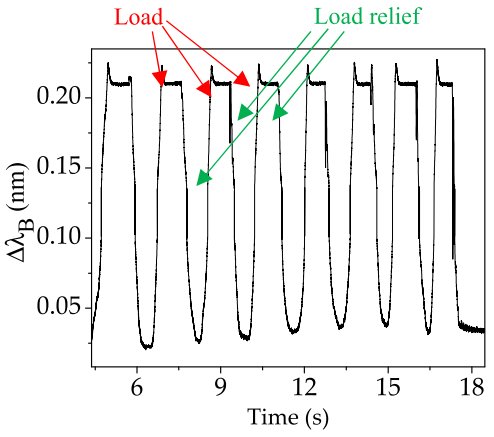

FIGURE 8. Determination of the response time and measurement repeatability of a sensor-cell.

1562 nm. One of the optical fiber cables is placed on the right side of the insole and has only the sensor-cell 4 (P4); the other fiber is on the left side and has the sensor-cells 1, 2 and 3 (P1, P2 and P3). Although it was possible to use only one optical fiber cable, we decided to use two optical fibers, and to multiplex the signal using an external 2 × 1 optical

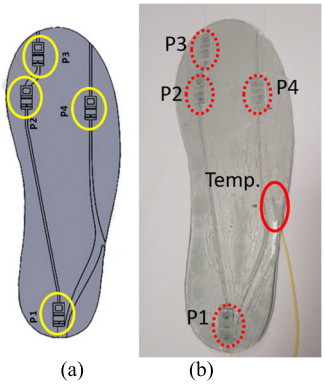

FIGURE 9. (a) Design of the insole PLA structure; (b) Instrumented insole with four sensor-cells and one temperature sensor.

coupler into 1 channel of the optical interrogator, aiming to avoid a tight curvature on the big toe, and consequently a signal attenuation.

Besides the PLA-base, the insole is composed by an epoxy resin layer (with a thickness of ≈1 mm) that provides strength, comfort, and protection to the optical fibers.

Figure 9b shows a picture of the insole after its instrumentation with the four sensor-cells. For simplicity, we adopted a nomenclature using a number and a letter. The 1, 2, 3 and 4 refer to the sensor-cell position, and the letters S and P concern to the shear and plantar forces. As example, 1S will represent the shear force for the sensor-cell in the position 1.

In order to evaluate the sensors temperature stabilization time, an FBG temperature sensor (FBG_T) was also adapted to the insole in order to monitor the temperature variations. This evaluation, prior to the insole implementation, shows that the Bragg wavelength shift registered during the gait cycles is the result of only the applied forces actuating on the sensor-cells, as no significant temperature variations occur after the stabilization period (Temp, Fig. 9b).

To determine the temperature stabilization time, FBG_T was monitored during 30 minutes with insole worn (Fig. 10). From the graph, it can be deduced that the value of the wavelength shift stabilizes after around 3 minutes.

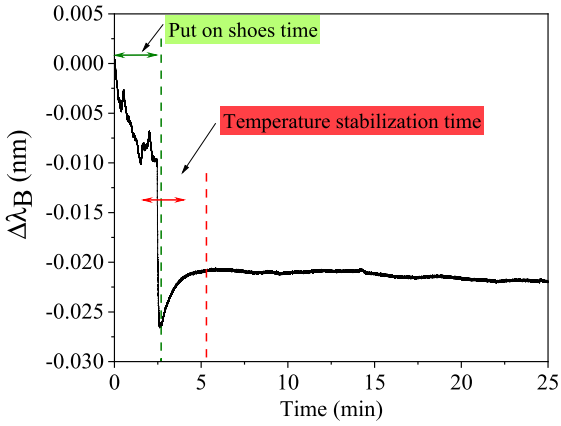

FIGURE 10. Determination of the temperature stabilization time.

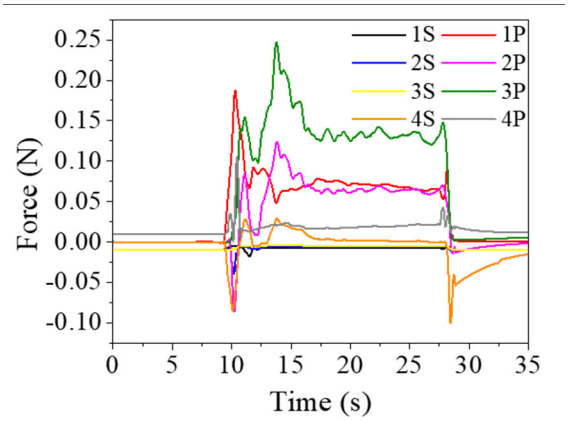

FIGURE 11. Instrumented insole's data acquired during the stability test of the center of mass.

The performance of the insole was first evaluated during a static test, in which one subject (female, 46 kg) remained static with the right foot supported on the entire surface of the insole, for about 20 s (Fig. 11). This test aims to evaluate the performance of the insole during the center of mass stability study, and to evaluate its response to plantar and shear force values.

The data presented in Fig. 11 can be analyzed by sections, according to the time/ evolution of the test and the respective stability of the center of mass: from 0 to 10 s is the time corresponding to the start of the test without any force applied to the insole; from 10 to 17 s is the allocation of the foot on the shoe with the insole and adjustment of the center of mass; from 17 to 28 s is the period that should be considered for analyzing the stability of the center of mass; and finally, the period after 28 s, corresponds to the insole exit.

By observing the data in Fig.11, it can be concluded that the sensors identified with the letter P (plantar) behave as expected: with positive Bragg wavelength shift, meaning that they have suffered positive vertical forces. We can also conclude that 3P was the zone that suffered the greatest force, which corresponds to the big toe area. The lowest value was registered for the 4P, which corresponds to the 4^{th} and 5^{th} metatarsal area. Regarding the sensors identified with the letter S (shear), their signal kept constant, with only visible changes in the process of placing and removing the foot in the insole, when a higher value of shear is also expected.

The tests were also carried out to evaluate the performance of the insole during the gait. For this, some slow steps were performed by the subject using the insole. It is important to note here that, this evaluation was only performed, after the insole were worn for 10 minutes, to ensure that the insole reaches the body temperature, thus minimizing the temperature influence. In Figure 12 it is represented four gait cycles acquired for the right foot during the insole performance evaluation. For graphical simplification, the timescale was reset to zero, close to the tests beginning.

As it can be seen in Fig. 12, in some locations (like P3), it is possible to clearly differentiate the plantar and the shear force

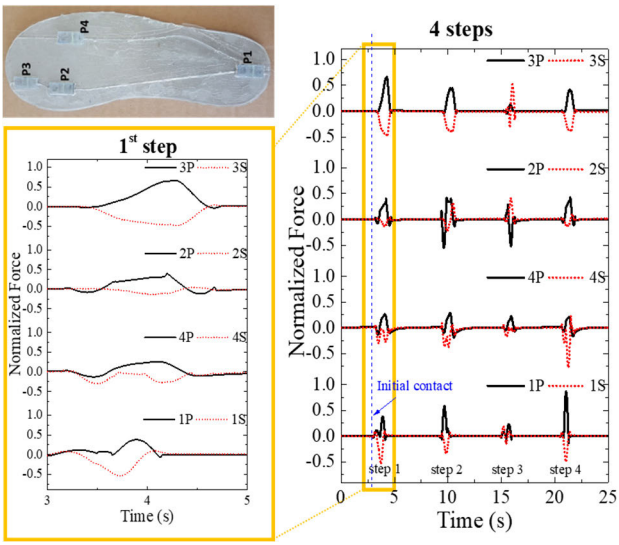

FIGURE 12. Behavior of the insole's four sensor-cells over four steps, with a zoom-in of the 1st step section, and with photograph of the instrumented insole to aid in the location of each sensor-cell in the insole.

exerted in the anteroposterior direction [14]. This location at the toe area is known to induce a more prominent effect of shear, right before the toe off moment of the gait cycle. Also, as expected by the design of the sensor-cell, the sensitivity of the FBG1 is greater when plantar forces are applied, whereas the sensitivity of the FBG2 is higher for shear forces.

It is also possible to verify that the shear forces recorded are more pronounced at the beginning, and at the end of each step, which is in accordance with expected behavior reported in the literature [16].

Regarding the total performance of the instrumented insole, it is in line with what would be expected in relation to the activation order of each sensor-cell: heel, followed by the metatarsal zones and finally the hallux [14], which also shows the good isolation between points of analysis.

V. OVERALL DEVICE ARCHITECTURE

The overall optically instrumented insole system comprises three components: the sensing element (insole), the interrogator system, and the mobile app on a smartphone (Fig. 13). The first component, the instrumented insole with optical fiber sensors (FBGs), has been substantially explained throughout the paper.

The second component is the interrogator system, required to acquire the signal modulated in the sensor-cells of the insole. The acquisition signal, in Bragg wavelength shift, can be translated into plantar and shear forces, using the proposed equations' system (3).

The third component is the mobile app designed for smartphones and/or tablets. This multiple functionality app is used as a data processing tool to analyze the values acquired from our system. It also displays the real-time results and statistics from the measured data over a period of time, when required by the patient (or doctor/caregiver). It may also be configured

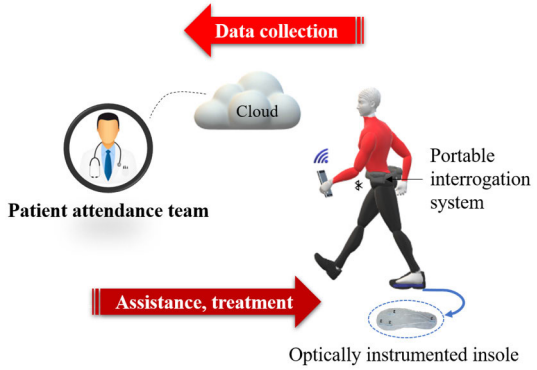

FIGURE 13. The overall optically instrumented insole system for gait plantar and shear force monitoring.

to provide alerts of critical force levels to the user, allowing to instantaneously correct the gait and body positioning. Finally, this app can also use the smartphone connectivity as a gateway for transmitting the results to a cloud. Thus, the medical team has continuous access to these data and may perform a more elaborate analysis of the patients' condition, allowing for better medical care.

The implementation of such architecture, which can be adapted to the sensors here presented, has been reported and detailed in [36].

VI. CONCLUSION

In this work, a reliable optical fiber based solution for real-time monitoring of the plantar and shear forces in different zones of an insole was proposed. The developed system consists of a mesh of sensor-cells positioned in four key-points to measure plantar and shear forces. Each sensor-cell is composed by two in-line FBGs, that can be multiplexed in a single optical fiber cable. For ease of assembly, in the case of the insole here reported, we used two optical fibers.

This work stands out from the previous ones for its ability to measure two forces applied simultaneously in different directions with the same sensor, with a high level of detail.

The presented architecture, based on the optical fiber technology, is a small, compact and reliable solution, with low complexity. Because conventional electronic sensors have some problems when used in this application field, which include their inoperability to be used in damp/humid environments and sensitivity to electromagnetic interferences, an alternative detection system is proposed.

An overall device architecture was also presented aiming to the development of a portable system with a mobile software application which offers the user the real-time visualization of the forces that are being applied at each of the key-points in the insole and to alert him if the values exceed the recommended ones. Therefore, the application of this optical sensing device, as an e-Health tool, can be advantageous for users who are likely to have problems with pressure ulcers, or other problems related to the foot and/or the spine.

REFERENCES

[1] V. Kontis, J. E. Bennett, C. D. Mathers, G. Li, K. Foreman, and M. Ezzati, "Future life expectancy in 35 industrialised countries: Projections with a Bayesian model ensemble," *Lancet*, vol. 389, no. 10076, pp. 1323–1335, Apr. 2017.

[2] M. Domingues, C. Tavares, C. Leitão, A. Neto, N. Alberto, C. Marques, P. Antunes, and P. André, "Insole optical fibre Bragg grating sensors network for dynamic vertical force monitoring," *J. Biomed. Opt.*, vol. 22, no. 9, pp. 91507–91515, 2017, doi: 10.1117/1.JBO.22.9.091507.

[3] C. Tavares, M. F. Domingues, T. Paixão, N. Alberto, H. Silva, and P. Antunes, "Wheelchair pressure ulcer prevention using FBG based sensing devices," *Sensors*, vol. 20, no. 1, p. 212, Dec. 2019, doi: 10.3390/s20010212.

[4] M. F. Domingues, C. Tavares, V. Rosa, L. Pereira, N. Alberto, P. Andre, P. Antunes, and A. Radwan, "Wearable eHealth system for physical rehabilitation: Ankle plantar-dorsi-flexion monitoring," in *Proc. IEEE Global Commun. Conf. (GLOBECOM)*, Waikoloa, HI, USA, Dec. 2019, pp. 9–13, doi: 10.1109/GLOBECOM38437.2019.9014293.

[5] M. F. Domingues, N. Alberto, C. S. J. Leitao, C. Tavares, E. R. de Lima, A. Radwan, V. Sucasas, J. Rodriguez, P. S. B. Andre, and P. F. C. Antunes, "Insole optical fiber sensor architecture for remote gait analysis—An e-health solution," *IEEE Internet Things J.*, vol. 6, no. 1, pp. 207–214, Feb. 2019, doi: 10.1109/JIOT.2017.2723263.

[6] M. Verbunt and C. Bartneck, "Sensing senses: Tactile feedback for the prevention of decubitus ulcers," *Appl. Psychophysiol. Biofeedback*, vol. 35, no. 3, pp. 243–250, Sep. 2010, doi: 10.1007/s10484-009-9124-z.

[7] H. Brem, J. Maggi, D. Nierman, L. Rolnitzky, D. Bell, R. Rennert, M. Golinko, A. Yan, C. Lyder, and B. Vladeck, "High cost of stage IV pressure ulcers," *Amer. J. Surg.*, vol. 200, no. 4, pp. 473–477, Oct. 2010, doi: 10.1016/j.amjsurg.2009.12.021.

[8] L. Wang, D. Jones, G. Chapman, H. Siddle, D. Russell, A. Alazmani, and P. Culmer, "A review of wearable sensor systems to monitor plantar loading," *IEEE. Trans. Biomed. Eng.*, vol. 67, no. 7, pp. 1989–2004, Dec. 2020, doi: 10.1109/TBME.2019.2953630.

[9] S. Rajala and J. Lekkala, "Plantar shear stress measurements—A review," *Clin. Biomech.*, vol. 29, no. 5, pp. 475–483, 2014, doi: 10.1016/j.clinbiomech.2014.04.009.

[10] C. Bayón, S. Lerma, O. Ramírez, J. I. Serrano, M. D. Del Castillo, R. Raya, J. M. Belda-Lois, I. Martínez, and E. Rocon, "Locomotor training through a novel robotic platform for gait rehabilitation in pediatric population: Short report," *J. Neuroeng. Rehabil.*, vol. 13, no. 1, pp. 98–104, Dec. 2016, doi: 10.1186/s12984-016-0206-x.

[11] D. Zou, M. J. Mueller, and D. J. Lott, "Effect of peak pressure and pressure gradient on subsurface shear stresses in the neuropathic foot," *J. Biomech.*, vol. 40, no. 4, pp. 883–890, Jan. 2007, doi: 10.1016/j.jbiomech.2006.03.005.

[12] T. W. Kernozek, E. E. LaMott, and M. J. Dancisak, "Reliability of an in-shoe pressure measurement system during treadmill walking," *Foot Ankle Int.*, vol. 17, no. 4, pp. 204–209, Apr. 1996, doi: 10.1177/107110079601700404.

[13] M. N. Orlin and T. G. McPoil, "Plantar pressure assessment," *Phys. Therapy*, vol. 80, no. 4, pp. 399–409, Apr. 2000, doi: 10.1093/ptj/80.4.399.

[14] A. Completo and F. Fonseca, *Fundamentos de Biomecânica Músculo-esquelÉtica e Ortopédica*. Porto, Portugal: Publindustria, 2011.

[15] A. Muro-de-la-Herran, B. Garcia-Zapirain, and Mendez-Zorrilla, "Gait analysis methods: An overview of wearable and non-wearable systems," *Sensors*, vol. 14, no. 2, pp. 3362–3394, 2014, doi: 10.3390/s140203362.

[16] A. H. A. Razak, A. Zayegh, R. K. Begg, and Y. Wahab, "Foot plantar pressure measurement system: A review," *Sensors*, vol. 12, no. 7, pp. 9884–9912, 2012, doi: 10.3390/s120709884.

[17] R. Correia, S. James, S.-W. Lee, S. P. Morgan, and S. Korposh, "Biomedical application of optical fibre sensors," *J. Opt.*, vol. 20, no. 7, Jul. 2018, Art. no. 073003, doi: 10.1088/2040-8986/aac68d.

[18] D. Tosi, E. Macchi, and A. Cigada, "Fiber-optic temperature and pressure sensors applied to radiofrequency thermal ablation in liver phantom: Methodology and experimental measurements," *J. Sensors*, vol. 2015, Jan. 205, Art. no. 909012, doi: 10.1155/2015/909012.

[19] A. Lekholm and L. Lindström, "Optoelectronic transducer for intravascular measurements of pressure variations," *Med. Biol. Eng.*, vol. 7, no. 3, pp. 333–335, May 1969, doi: 10.1007/BF02474776.

[20] B. He, M. Li, J. Chen, W. Guo, G. Xu, and J. Xie, "An intensity-modulated fiber optic pressure sensor for hand-exoskeleton interactive force detection," in *Proc. 16th Int. Conf. Ubiquitous Robots (UR)*, Jeju, South Korea, Jun. 2019, pp. 750–754, doi: 10.1109/URAI.2019.8768686.

[21] D. Jia, J. Chao, S. Li, H. Zhang, Y. Yan, T. Liu, and Y. Sun, "A fiber Bragg grating sensor for radial artery pulse waveform measurement," *IEEE Trans. Biomed. Eng.*, vol. 65, no. 4, pp. 839–846, Apr. 2018, doi: 10.1109/TBME.2017.2722008.

[22] T. Allsop, K. Carroll, G. Lloyd, D. J. Webb, M. Miller, and I. Bennion, "Application of long-period-grating sensors to respiratory plethysmography," *J. Biomed. Opt.*, vol. 12, no. 6, 2007, Art. no. 064003, doi: 10.1117/1.2821198.

[23] A. V. Koulaxouzidis, M. J. Holmes, C. V. Roberts, and V. A. Handerek, "A shear and vertical stress sensor for physiological measurements using fibre Bragg gratings," in *Proc. 22nd Annu. Int. Conf. IEEE Eng. Med. Biol. Soc.*, Jul. 2000, pp. 23–28, doi: 10.1109/IEMBS.2000.900666.

[24] Z. F. Zhang, X. M. Tao, H. P. Zhang, and B. Zhu, "Soft fiber optic sensors for precision measurement of shear stress and pressure," *IEEE Sensors J.*, vol. 13, no. 5, pp. 1478–1482, May 2013, doi: 10.1109/JSEN.2012.2237393.

[25] K. Chethana, A. Prasad, S. Omkar, and S. Asokan, "Design and development of optical sensor based ground reaction force measurement platform for gait and geriatric studies," *Int. J. Mech. Mechatron. Eng.*, vol. 10, no. 1, pp. 60–64, 2016, doi: 10.5281/zenodo.1338606.

[26] M. Domingues, C. Tavares, C. Leitão, A. Neto, N. Alberto, C. Marques, A. Radwan, J. Rodriguez, O. Postolache, E. Rocon, P. André, and P. Antunes, "Insole optical fiber Bragg grating sensors network for dynamic vertical force monitoring," *J. Biomed. Opt.*, vol. 22, no. 9, p. 91507, 2018, doi: 10.1117/1.JBO.22.9.091507.

[27] D. Vilarinho, A. Theodosiou, C. Leitão, A. Leal-Junior, M. Domingues, K. Kalli, P. André, P. Antunes, and C. Marques, "POFBG-embedded cork insole for plantar pressure monitoring," *Sensors*, vol. 17, no. 12, p. 2924, 2017, doi: 10.3390/s17122924.

[28] C. Tavares, M. Domingues, A. Frizera-Neto, C. Leitão, N. Alberto, C. Marques, A. Radwan, E. Rocon, P. André, and P. Antunes, "Biaxial optical fiber sensor based in two multiplexed Bragg gratings for simultaneous shear stress and vertical pressure monitoring," *Proc. SPIE*, vol. 10680, May 2018, Art. no. 106802R, doi: 10.1117/12.2306889.

[29] C. Tavares, M. Domingues, A. Frizera-Neto, T. Leite, C. Leitão, N. Alberto, C. Marques, A. Radwan, E. Rocon, P. André, and P. Antunes, "Gait shear and plantar pressure monitoring: A non-invasive OFS based solution for e-health architectures," *Sensors*, vol. 18, no. 5, p. 1334, 2018, doi: 10.3390/s18051334.

[30] C. Tavares, M. Domingues, N. Alberto, A. Ramos, E. Rocon, P. André, H. Silva, and P. Antunes, "Bioinspired optical fiber sensor for simultaneous shear and vertical forces monitoring," *Proc. SPIE*, vol. 11028, Apr. 2019, Art. no. 110282M, doi: 10.1117/12.2522330.

[31] O. Al-Mai, J. Albert, and M. Ahmadi, "Development and characterization of compliant FBG-based, shear and normal force sensing elements for biomechanical applications," *IEEE Sensors J.*, vol. 20, no. 10, pp. 5176–5186, May 2020, doi: 10.1109/JSEN.2020.2969866.

[32] E. A. Al-Fakih, N. B. Arifin, G. Pirouzi, F. R. M. Adikan, H. N. Shasmin, and N. A. A. Osman, "Optical fiber Bragg grating-instrumented silicone liner for interface pressure measurement within prosthetic sockets of lower-limb amputees," *J. Biomed. Opt.*, vol. 22, no. 8, Aug. 2017, Art. no. 087001, doi: 10.1117/1.JBO.22.8.087001.

[33] J. R. Galvão, C. R. Zamarreño, C. Martelli, J. C. D. Silva, F. J. Arregui, and I. R. Matías, "Smart carbon fiber transtibial prosthesis based on embedded fiber Bragg gratings," *IEEE Sensors J.*, vol. 18, no. 4, pp. 1520–1527, Feb. 2018, doi: 10.1109/JSEN.2017.2786661.

[34] L. Armitage, G. Rajan, L. Kark, A. Simmons, and B. G. Prusty, "Simultaneous measurement of normal and shear stress using fiber Bragg grating sensors in prosthetic applications," *IEEE Sensors J.*, vol. 19, no. 17, pp. 7383–7390, Sep. 2019, doi: 10.1109/JSEN.2019.2914702.

[35] T. Leite, "Optical fiber solutions to physical rehabilitation systems and e-health applications," Univ. Aveiro, Aveiro, Portugal, Tech. Rep., 2018, pp. 616–718, vol. 535.

[36] J. Monge, O. Postolache, R. Alexandre, M. F. Domingues, and P. V. A. Viegas, "Fiber Bragg gratings solution for gait assessment," in *Proc. IEEE Int. Instrum. Meas. Technol. Conf. (IMTC)*, Dubrovnik, Croatia, May 2020, pp. 1–6.

CÁTIA TAVARES was born in Aveiro, Portugal, in July 1992. She received the master's degree in physics engineering from the University of Aveiro, Portugal, in 2016. She currently holds a DAEPHYS Ph.D. scholarship at Physics Department, Institute of Nanostructures, Nanomodelling and Nanofabrication, University of Aveiro. Her current research interest includes the development of optical fiber sensors for e-Health solutions.

FLÁVIA LEITE is currently pursuing the integrated master's degree in biomedical engineering with the University of Aveiro. Her research interests include projects in biomedical engineering area, namely in optical biosensors and medical imaging.

MARIA DE FÁTIMA DOMINGUES (Member, IEEE) received the M.Sc. degree in applied physics and the Ph.D. degree in physics engineering from the University of Aveiro, Portugal, in 2008 and 2014, respectively. In 2015, she held a research fellow position with the Instituto de Telecomunicações–Aveiro and the Consejo Superior de Investigaciones Científicas (CSIC), Madrid, Spain. She is currently a Researcher with the Instituto de Telecomunicações–Aveiro. She has authored or coauthored more than 80 journals and conference papers, several book chapters, and two books. Her current research interests include solutions of optical fiber-based sensors and its application in robotic exoskeletons and e-Health scenarios, with a focus in physical rehabilitation architectures.

TIAGO PAIXÃO received the B.S., M.S., and Ph.D. degrees in physics engineering from the University of Aveiro, Portugal, in 2014, 2016, and 2021, respectively. From 2016 to 2017, he was a Research Fellow with the Institute for Nanostructures, Nanomodelling and Nanofabrication (I3N) and the Telecommunications Institute (IT), Aveiro, Portugal. He is currently a Researcher with I3N and the University of Aveiro. His research interests include the development, optimization, and application of new optical fiber sensing architectures, based on fiber gratings and interferometers produced by nano and femtosecond lasers, to monitor physical and chemical parameters.

NÉLIA ALBERTO received the Ph.D. degree in physics from the University of Aveiro, Portugal, in 2011.

From 2012 to 2017, she worked under an FCT Postdoctoral Research Fellowship. In 2018, she was hired as a Researcher by the Instituto de Telecomunicações, Aveiro, Portugal. She has acquired expertise in the design and development of optical fiber sensors, fiber coatings, and application in different contexts, with special focus for medical environments. She is the author or coauthor of six book chapters, 44 articles in international peer-reviewed journals, and more than 60 papers in conference proceedings.

ANTÓNIO RAMOS received the Ph.D. degree in mechanical engineering from the University of Aveiro, Portugal, in 2005. From 2007 to 2019, he worked as a Researcher with TEMA–Aveiro, Portugal. His research interests include the study of medical devices, including long-term behavior focused in bone implant interaction, using experimental and computational model to predict the behavior and other field is product development in medical devices and clean energy.

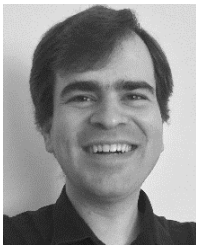

HUGO SILVA (Senior Member, IEEE) received the Ph.D. degree in electrical and computer engineering from the Instituto Superior Técnico (IST), University of Lisboa (UL). He has been a Researcher with the Instituto de Telecomunicações, since 2004. He has been a Co-Founder of multiple technology-based healthcare companies, since 2007. He is currently a Professor with the Instituto Superior Técnico, Universidade de Lisboa (IST-UL). His current research interests include biosignal research, systems engineering, signal processing, and pattern recognition. His work has been internationally distinguished with several academic and technical awards.

PAULO FERNANDO DA COSTA ANTUNES received the B.Sc. degree in physics engineering, the M.Sc. degree in applied physics, and the Ph.D. degree in physics engineering from University of Aveiro, Aveiro, Portugal, in 2005, 2007, and 2011, respectively. From 2017 to 2019, he was an Assistant Researcher with the Physics Department, Institute of Nanostructures, Nanomodelling and Nanofabrication (I3N), University of Aveiro. He is currently an Assistant Professor with the Department of Physics, University of Aveiro, and a Researcher with I3N and the Telecommunications Institute (IT). His research interests include the study and simulation of optical fiber sensors based on silica and polymeric fibers, for static and dynamic measurements, data acquisition, optical transmission systems, and sensor networks for several applications, such as temperature and strain measurements in extreme environments, structural monitoring, physical rehabilitation, and among others.